Cytotechnology (2013) 65:119–134
DOI 10.1007/s10616-012-9467-9

ORIGINAL RESEARCH

Improving the attachment and proliferation of umbilical cord mesenchymal stem cells on modified polystyrene by nitrogen-containing plasma

Somruthai Tunma · Kewalin Inthanon · Chanokporn Chaiwong · Jantrawan Pumchusak · Weerah Wongkham · Dheerawan Boonyawan

Received: 1 December 2011 / Accepted: 21 May 2012 / Published online: 4 July 2012
© Springer Science+Business Media B.V. 2012

Abstract Wharton's jelly mesenchymal stem cells (WJMSCs) are important alternative source of pluripotent cells for several therapeutic purposes. Understanding of adhesion properties of such cells is necessary to regulate the attachment, growth and proliferation on targeted culture surfaces. BCP-K1, a line of WJMSCs, and polystyrene (PS) culture dishes were used as membrane samples. A 13.56 MHz inductively coupled discharge plasma reactor with a mixture of N-containing gas and noble gas was used. This was expected to introduce the more hydrophilic groups on PS surface and enhance the cell adhesion. The plasma-treated PS dishes with the mixed gas of N_2 + He at 50 W and NH_3 + He at 100 W were reactive towards BCP-K1. Cellular adhesion and proliferation was significantly twice as efficient on the treated surfaces than on PS dishes. BCP-K1 also secreted more focal adhesion kinase to adhere and proliferate when cultured on N_2-treated PS dishes than on the NH_3-treated PS dishes. Stable stemness markers were detected, including CD105, CD9 and SSEA-4, expressed on BCP-K1 growing on the modified PS dish surfaces, during 7 days of culturing. The presence of $-NH_2$ groups on the PS dish surface were revealed by X-ray photoelectron spectroscopy and Fourier transform infrared spectroscopy. A large amount of oxygen- and nitrogen-containing functional groups, up to 9.0 %, were introduced by NH_3 plasma and N_2 plasma. The functional groups introduced on to the PS surfaces were clearly the key factors which enhanced WJMSCs attachment and stemness stability.

Keywords Umbilical cord · Wharton's jelly mesenchymal stem cells (WJMSCs) · FAK · Proliferation · Stemness regulation · Polystyrene (PS) culture dish · N-containing plasma

S. Tunma · K. Inthanon
The Graduate School, Chiang Mai University, 239 Huaykaew Rd., Muang 50200, Thailand

S. Tunma · J. Pumchusak · D. Boonyawan
Materials Science Research Center (MSRC) Faculty of Science, Chiang Mai University, 239 Huaykaew Rd., Muang 50200, Thailand

K. Inthanon · W. Wongkham (✉)
Department of Biology, Faculty of Science, Chiang Mai University, 239 Huaykaew Rd., Muang 50200, Thailand
e-mail: weerah.w@cmu.ac.th

C. Chaiwong · D. Boonyawan
Department of Physics and Materials Science, Faculty of Science, Chiang Mai University, 239 Huaykaew Rd., Muang 50200, Thailand

J. Pumchusak
Department of Industrial Chemistry, Faculty of Science, Chiang Mai University, 239 Huaykaew Rd., Muang 50200, Thailand

Introduction

Cell therapy, using mesenchymal stem cells (MSCs), can be used to treat many human diseases. This can be achieved by the transplantation of cells, in sufficiently high numbers and quality, to a damaged target organ. The cells must then survive long enough to restore normal function. Requirements for culture-vessel surface optimization are evolving according to the types of cell used. To meet these demands, it is necessary to increase understanding of the biological mechanisms of cellular adhesion, to optimize physicochemical properties of biomaterial surfaces and the cellular culture microenvironment. Most of the commercialized-designed surfaces are well developed for common types of cells in culture, but more specific cell types require more advanced modifications. MSCs from different sources, such as bone marrow cavity, so called BMSCs, umbilical cord blood, CBMSCs, or umbilical cord Wharton's jelly, WJMSCs have been identified as a highly potential of similar differentiation (Baksh et al. 2008; Troyer and Weiss 2008). However, several reports using these MSCs mentioned their poor adhesive capability or reduced attachment capacity following culture expansion on the available commercialized culture vessels (Zhang et al. 2007; Prockop 2004; Barbash et al. 2003; Chen et al. 2001). Different adhesive characteristics were found with cells from different origin (Wagner et al. 2005; Sarugaser et al. 2005; Koh et al. 2008; Docheva et al. 2007). Despite the high potential of application for WJMSCs, very little research has been done to increase understanding of adhesion capacity on modified surface of different types (Ji et al. 2009; Baksh et al. 2007).

Polystyrene (PS) has been used since 1965 (Rubin 1966) as a popular culture vessel material for microbes, due to its excellent durability, transparency and non-toxicity. PS itself is unsuitable for eukaryotic cell culture, because of its hydrophobic nature. Therefore, surface treatments are required to optimize cell adhesion (Grinnell 1978; Maroudas 1977; Amstein and Hartman 1975; Skarlatos et al. 1992). Modified surfaces, using plasma-treated PS surfaces can improve cell proliferation, expand cell adhesion and increase cell yields (Van Kooten et al. 2004; Teare et al. 2000; Dupont-Gillain et al. 2000). Addition of inert gases such as argon (Ar), neon (Ne) and helium (He) in nitrogen plasma, enhances the concentration of active species through Penning excitation and ionization processes (Veronis et al. 2000; Hiraoka et al. 2004). He has higher metastable energies than any other inert gas. This making it a powerful Penning reagent for exciting plasma species through inelastic collisions, and thus can be added in nitrogen-containing plasma to achieve a considerable increase in the reactive level (Bell et al. 1968; Kubota 1970). He or Ar gas are commonly used in the laboratory because of their low cost, whereas Ne, xenon (Xe), and other noble gases are of limited application. Most of the present commercialized PS culture vessels are normally pretreated, using variety of techniques including corona discharge, ultraviolet radiation, gamma irradiation and gas plasma modification (Granchelli 2009). These techniques provide hydrophilicity to PS surfaces either by oxidizing and chemical functional group alteration. This is a consequential factor defining the surface energy, polarity, wettability and zeta potential, and accordingly the character of the cell-material interaction. There is optimal cell adhesion to temperately hydrophilic and positively charged substrates, because of the adsorption of cell adhesion-mediating molecules accessible to cell adhesion receptors (e.g., integrins). Cell adhesion to positively charged surfaces is better than to negatively charged surfaces. The reasoning is that the cell surfaces adhesive-molecules are negatively charged and consequently adhere preferentially to positively charged surfaces (Bacakova et al. 2011). The hydrophilic and protein-containing (extracellular matrix molecules) surfaces are known to be good for cell growth. Because the amine group ($-NH_2$) is positively charged, it is highly reactive and therefore covalently couples proteins in aqueous environments (Birgit et al. 2007; Truica-Marasescu et al. 2008; Bacakova et al. 2011; Kim et al. 2006; Ronald et al. 1995). Although, these surface properties are well understood, among a broad spectrum of different cell types, they are not well defined for WJMSCs.

Therefore, we studied the reactions of WJMSCs on the nitrogen-containing plasma, used to deposit amine functional groups onto PS dish surfaces. The process was performed in a mixed gas of N_2 or NH_3 and He or Ar, in order to understand which kinds of mixed gas and the optimum power play an important role in the control of reactions between surface reactive species and plasma reactive species. Previous studies showed that the concentration of functional groups, introduced on a polymer surface by plasma treatments, may change over time, depending on the environment and temperature, especially amine functional groups (Kim et al. 2006; Ronald et al. 1995). In this study we focus on the long-term effect of physico-chemical properties of the noble gas mixture on enhancement of reactive species in nitrogen-containing plasma and on hydrophobic recovery of treated PS surfaces over 30 days. Hydrophobic recovery means surface restructuring of the polymer, a reorientation of nonpolar groups (hydrophobic property) from the bulk to the surface and condensation of surface hydroxyl groups.

Materials and methods

Deposition surfaces were characterized by Fourier transform infrared (FTIR) spectroscopy, X-ray photoelectron spectroscopy (XPS) and water contact angle measurement. We also investigated the short-term effect, over 7 days, on cellular behavior including attachment (adhesion), proliferation rate and stemness of WJMSCs on plasma-treated PS surfaces compared with commercial oxygen-containing pretreated PS culture dishes.

PS sample preparation

Commercial PS culture dishes (Nunclon®, Roskilde, Denmark; Cat#153066), 35 mm in diameter, were used as the material model in this study. The bottom part of each dish was carefully cut free from its surrounding high edge to obtain a circular PS-membrane sample, 14 mm in diameter, using a stainless-blade, mounted on a motor-operated instrument. The sample membranes were carefully handled before, during and after the cutting process to prevent fingerprints and any other surface disrupting dirt. After being cut, these sample membranes were cleaned in ethanol with ultrasonic for 5 min and sterilized in a plasma chamber (Yasushi et al. 2008). They were used in this experiment as re-treated PS (NH_3-treated PS or N_2-treated PS) with the assigned plasma gases. In our experiments, the PS-membrane samples were randomly separated into 2 groups; the first group for the long-term 30 days course of physico-chemical evaluation and the second for the short-term 7 days course, with the WJMSCs interaction studies.

The PS-control material for the cell bioassay was the surface of 24-well-bottom plates, pretreated commercially with oxygen (Nunclon®, Denmark; Cat#142475). The plates used were the originally sterilized products from the producer.

Physico-chemical properties study

PS-membrane samples were treated and evaluated by the following techniques.

Plasma treatment

To manipulate the re-treated PS-membrane, a self-made inductively-coupled discharge plasma system operated at 13.56 MHz (as described by Chaiwong et al. 2010) was employed to treat the samples. The original pretreated PS-membrane samples were introduced into a chamber, which was evacuated by a rotary pump to a base pressure of 2.1 Pa. The samples were cleaned by Ar plasma sputtering for 10 min before treatment. Nitrogen-functional groups were deposited onto the PS-membrane surface, using a mixture of noble gas (He and Ar) and nitrogen-containing gas (N_2 and NH_3). The total pressure of the gas mixture was kept constant at 13.33 Pa. The ratio of N_2 and NH_3 to He or Ar was fixed at 10 % by volume. The deposition process was carried out at an RF power of 50 and 100 W for 15 min.

Evaluation

Contact angle was obtained using the sessile drop technique with DI water droplet of 10 µl. A micropipette was used to drop the water on the surface of PS-membrane samples. The image of the water droplet was then captured and exported to an image analyzing software to determine the contact angle. Water contact angle measurement demonstrates the relationship between the properties and chemistry of a surface by wettability. The contact angle (in °) is the angle at which a liquid interface meets a solid surface. The greater the angle, the higher is the surface hydrophobicity.

An ATR-unit of a Nicolet 6700 FTIR spectrophotometer (Bruker, Germany) was used to investigate chemical bonding on the sample surfaces. The spectra were collected by averaging 64 scans at a resolution of 4 cm^{-1} from 400 to 4,000 cm^{-1}.

X-ray photoelectron spectroscopy was carried out to determine the quantitative and qualitative elemental surface composition, using an Ultra DLD spectrometer (Kratos Analytical Ltd., UK) with a monochromatized Al–K_α X-ray source ($h\nu$ = 1,486.6 eV). The anode voltage and current were 15 kV and 10 mA.

Survey spectra were collected using a pass energy of 160 eV with 1 eV/step, while region scans were collected with a pass energy of 40 eV, at a rate of 0.1 eV/step. The pressure in the analysis chamber was maintained at 7×10^{-7} Pa. Binding energy was referenced to the C1s neutral carbon peak at 284.6 eV.

Cell behavior study

Two treated PS-membrane types were compared with the PS-control group. The chosen criterion was mainly considered on the highest attachment efficiency of the cells at day 1.

Cell culture and seeding

The BCP-K1, a line of WJMSCs, was provided from The Human and Animal Cell Technology Research Laboratory, Department of Biology, Faculty of Science, Chiang Mai University. The cells were cultured on 25 cm^2 pretreated PS cultured flasks (Nunclon®, Roskilde, Denmark; Cat#156340) in DMEM (Dulbecco's modified Eagle's medium) (Gibco, Grand Island, NY, USA) containing 20 % (v/v) FBS (fetal bovine serum) (Gibco), 10 ng/ml bFGF (basic fibroblast growth factor) (Sigma, St, Louis, MO, USA) and 5 mg/ml bovine insulin (Sigma, USA). Cultures were maintained at 37 °C, 5 % CO_2 and 95 % relative humidity. The culture medium was refreshed every 2 days before achieving 80 % cell-population confluence. On detaching from the cultured flasks, they were exposed to 0.05 % (v/v) trypsin–EDTA (Gibco, USA) for 10 min. The cells were collected and washed with phosphate buffer saline (PBS) then centrifuged and resuspended in the medium prior to cell seeding. The cells were counted and the cell density adjusted to 30,000 cells/ml. Then the cells were seeded onto each PS-membrane sample, which was previously settled on the bottom of each well of a 24-well PS culture plate. The diameter size of a PS-membrane sample was actually made to match and set onto the diameter of a well on this 24-well culture plate. Cell attachment and proliferation were evaluated 1, 3, 5 and 7 days after seeding. The experiment was performed in 5 replicates of the same type of PS-membrane sample. Similar cell density, culture conditions, replications and evaluated periods were carried out on the PS-control 24-well-bottom plates.

Cell attachment efficiency and proliferation assay

Attachment efficiency and proliferation assay of BCP-K1 were quantitatively evaluated by using the Vybrant® MTT Cell Proliferation Assay Kit (Molecular Probes, Leiden, the Netherlands). The PS-membrane samples containing attached cells, were transferred to a new 24-well plate, filled with 500 μl fresh medium in each well. This was to avoid false evaluation on the cells overflown from PS-membrane samples. The assay for cells on PS-control groups was performed in the initial 24-wells culture plate (no transfer). According to the manufacture's instruction, 50 μl MTT-solution was added to each well (final concentration 0.5 mg/ml) and incubated at 37 °C for 4 h. Thereafter, 500 μl of the solubilization mixture (1 g SDS: 0.1 M HCl) was added into each well to dissolve formazan crystals, produced by active cells, and left overnight at 37 °C. The colorimetric optical density (OD) of liquid in each well was obtained by spectrophotometry at 570 nm using Spectra™ MR Microplate Spectrophotometer (Dynex Technologies, Chantilly, VA, USA). The proliferation assay was analyzed using the OD_{570} value from each PS membrane sample at various culture periods in comparison to the control at day 1, which was presented as percentage of attached and proliferated cells. A higher percentage of cell attachment and proliferation corresponds to a higher number of viable cells.

FAK-ELISA

FAK (focal adhesion kinase) was assessed using the enzyme-linked immunosorbent assay (ELISA) method to measure an anchorage-dependent protein in cells, which adhered on each PS-membrane sample. After seeding cells onto PS-membrane samples, the FAK-ELISA was performed at every time period, at 1, 3, 5 and 7 days, as mentioned above. Each sample was washed with PBS for 2–3 times prior to fixation by 4 % (v/v) formaldehyde for 20 min at room temperature. The sample was washed twice thereafter with washing buffer (0.1 % (v/v) Triton X-100 in PBS) then incubated with the quenching buffer (wash buffer containing 1 % (v/v) H_2O_2 and 0.1 % (v/v) Azide) for 30 min and washed with washing buffer. Blocking buffer [5 % (v/v) BSA (bovine serum albumin) (Invitrogen, Carlsbad, CA, USA)] was added for 1 h before adding anti-FAK primary antibody (1:2,000) (Sigma) and incubated at 4 °C overnight. The HRP (horseradish peroxidase)-labeled secondary antibody (1:20,000) was added in each sample, incubated for 2 h. The SIGMA*FAST*™ OPD (o-phenylenediamine-dihydrochloride) (Sigma), a substrate for HRP, was added to the samples then incubated for 30 min in the dark to allow color development. The samples were then measured at OD_{492} nm, using a microplate spectrophotometer as described previously.

Immunocytochemical analysis

Immunocytochemistry was carried out on the 3 groups of BCP-K1 growing on PS surfaces as mention in the short-term cell behavior study. Cells were examined at the initial stage (day 1) and when the experiment finished (day 7). The method was adapted from Brohlin et al. (2009). In brief, cells on a PS-membrane surface were rinsed with 1x PBS (pH 7.4), followed by fixation with 4 % formaldehyde in PBS for 15 min. The cells were then washed 3 times with PBS and permeabilized with 0.1 % Triton X-100 in PBS in 37 °C for 30 min followed by 10 min at room temperature. The cells were gently washed 3 times with PBS at room temperature and blocked in 10 % Bovine Serum Albumin (BSA; Invitrogen) for 1 h at room temperature in humidified container. Cells were then incubated overnight at 4 °C with mouse monoclonal antibody for human CD105 (1:2,000), human CD34 (1:2,000), SSEA-4 (1:2,000) (all from Molecular Probes, Invitrogen) and human CD9 (1:500) (US biological, Swampscott, MA, USA). After rinsing in PBS for 3 times, secondary goat anti-mouse antibodies Alexa Fluor® 488 goat anti-mouse IgG_1 (1:200), Alexa Fluor® 594 goat-anti mouse $IgG_3(\gamma3)$ (1:200) and Alexa Fluor® 546 goat anti-mouse $IgG_{2b}(\gamma2b)$ (1:200) (all from Molecular Probes), were added and incubated for 1 h at room temperature in the dark. Cells were washed a further three times in PBS and incubated in 300 nM 4′,6-diamidino-2-phenylindole (DAPI) and mounted with ProLong® Gold anti-fade reagent (both from Molecular Probes). The mounted and stained cells were allowed to cure for 24 h at room temperature in the dark before photomicrography under an epifluorescent microscope (Olympus DP-50, Olympus, Tokyo, Japan).

Cell morphology

Cell morphology was observed under a light microscope equipped with digital photomicrography devices. A scanning electron microscope (SEM) (JSM 633S Jeol, Tokyo, Japan) was also used to observe the fine details of the attachment mechanism of cells on the surfaces.

Data analysis

All data were presented as mean ± SD. Analysis of differences in the means between different PS-membrane samples and controls were performed by the One-Way ANOVA procedure, followed by multiple comparisons using Duncan adjustment at $p \leq 0.01$.

Results and discussion

Surface wettability and aging effect of plasma treated-PS

The surface hydrophilicity of treated PS-membrane was significantly improved in both N_2 and NH_3 plasma treatments (Table 1). Treated samples had a considerably lower contacted angle of 20° (compared with 82.8° for the PS-control), indicating good spreading of water on the material surface and low hydrophobicity of the material surface. The nitrogen-containing plasma treated PS-membrane were more hydrophilic, resulting in more polar groups ($–NH_2$ and oxidized structures e.g., carbonyl, carboxyl and ester groups) being grafted onto the surface during the plasma treatment (Birgit et al. 2007; Lizhen et al. 2010; Chaiwong et al. 2010). Nonpolar molecules are exhibited by London forces because of the correlated movements of the electrons in interacting molecules.

Table 1 Water contact angle of PS-control and plasma treated PS-membrane

Nitrogen-containing plasma	Contact angle (°) ± SD
Control PS	82.8 ± 1.4
10 % N_2 + Ar, 50 W	20.1 ± 5.8
10 % N_2 + Ar, 100 W	17.5 ± 3.6
10 % N_2 + He, 50 W	14.3 ± 2.6
10 % N_2 + He, 100 W	13.4 ± 5.0
10 % NH_3 + Ar, 50 W	17.3 ± 2.0
10 % NH_3 + Ar, 100 W	11.1 ± 1.5
10 % NH_3 + He, 50 W	13.4 ± 3.5
10 % NH_3 + He, 100 W	14.6 ± 4.1

These forces reveal weak intermolecular forces. If the material is too hydrophobic, molecules of extracellular matrix (ECM) are absorbed in a denatured and rigid state. This geometrical appearance is unsuitable for binding to cells, since specific sites on these molecules are less accessible to cell adhesion receptors, e.g., integrin. The polar component of surface energy consists of all other interactions due to non-London forces. Polar molecules interact through dipole–dipole intermolecular forces and hydrogen bonds (Bacakova et al. 2011). On hydrophilic surfaces, cells adhered in higher numbers to more hydrophilic materials and were spread over a large area. At the same time, ECM proteins were adsorbed in a more flexible form, which allows them to be rearranged by the cells and thus provides access for cell adhesion receptors to the adhesion motifs on these molecules.

The incorporated amine groups are capable of efficient interaction with ECM proteins by hydrogen bonding, resulting in covalent attachment between the positively charged groups (–NH_2) and the cells that carry a negative charge (Birgit et al. 2007; Truica-Marasescu et al. 2008).

However, in many cases the amine surfaces had a rather limited shelf life after plasma oxidation reactions. When the plasma-treated surface was preserved at elevated temperature or storage in air, the contact angle increased greatly. In other words, an increase in the hydrophobicity of the surface, due to improper storage temperature and atmosphere, allowed the reorientation of the hydrophobic group (hydrophobic recovery) of the surface and subsurface layers to become dominant (Kim et al. 2000). Contact angle and X-ray photoelectron spectroscopy revealed that this hydrophobic recovery is influenced by aging condition.

The stability of a plasma-treated polymer surface is an important issue for biomedical use. Structural elements (chains and chain segments) can move between polymer surfaces and deeper layers (bulk) by rotational and translational motions. The surface composition can change to minimize the interfacial energy between the polymer and its environment (Gerritsen et al. 1995). Figure 1 shows decay of wettability over 30 days after N_2 and NH_3 plasma treatments. The contact angle of treated-PS surfaces with higher rf power (100 W) were lower than that of 50 W rf power treated-surfaces. Moreover, the decay of 100 W Rf power treated-surfaces was less than of 50 W Rf power treated-surfaces. It can be concluded

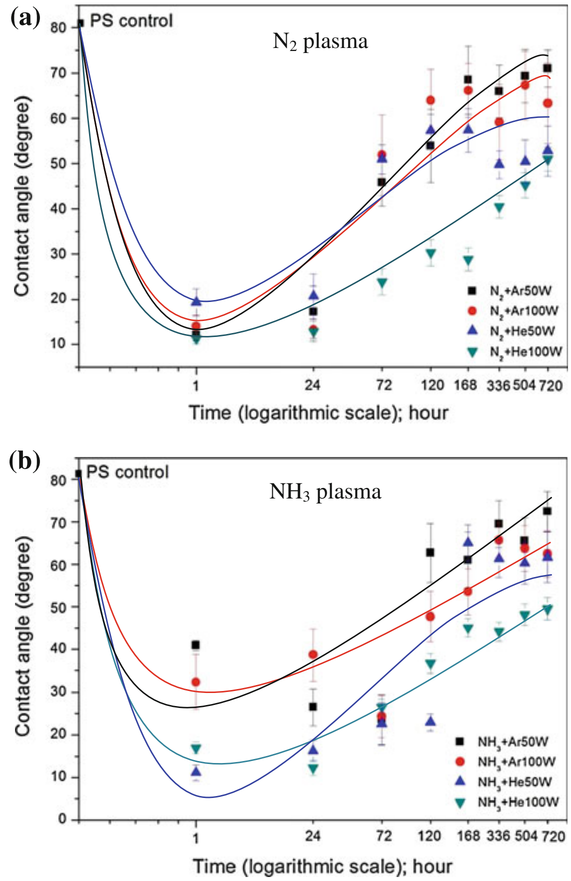

Fig. 1 Decay of wettability of PS surfaces over 30 days after N_2- (**a**) and NH_3-plasma treatment (**b**)

that the optimum Rf power for mixed gases of He and N_2 or NH_3 was 100 W.

In Fig. 1a, the decay of N_2 + He plasma treated surface was lower than that of N_2 + Ar plasma treated surface. Similarly, in Fig. 1b the decay of NH_3 + He plasma treated surface was also lower than that of NH_3 + Ar plasma treated surface. Therefore it is suggested that He gas plasma can be used to create stable covalent binding sites for the attachment of amine functional groups over a long time. Inert gas plasma treatments introduce no new detectable chemical species onto the polymer surface, but they can induce degradation and rearrangement of the polymer surface. During inert gas plasma exposure, the created functional sites produces dangling bonds (by removal of H atoms and breaking chemical bonds in polymer chains), which may recombine to cross-link neighboring polymer chains (Ronald et al. 1995; Yuk-Hong et al. 2010; Junyou et al. 2005). He plasma is well known to efficiently produce cross-linking reactions (Yuk-Hong et al. 2010; Naveed et al. 2006). We expected that the formation of a cross linked polymer surfaces, preventing reptation of the modified polymer chains into the bulk, could be the reason for the improved stability observed for the mixed He gas-treated plasma (Naveed et al. 2006). Coating the PS surface with Ar, before reaction with an N containing plasma, extracts H from C–H bonds, creating functional sites, which rupture polymer chains. The functional sites subsequently couple with free radical sites, with active species from the N-containing plasma phase, to form N-containing functional groups (Ronald et al. 1995; Yuk-Hong et al. 2010; Riccardi et al. 2010). Reactive gas plasma (e.g., NH_3, N_2, O_2 CF_4 and SF_6) treatments create new chemical species, which bring about chemical reactivity of the polymer surface (Arefi-Khonsari et al. 1995). However, the most important surface population of chemical species, formed after plasma treatment, is dependent on both the chemical structure of the polymer and the plasma gas.

Surface characterization

For FTIR analysis, the plasma-treated PS membranes have been characterized by ATR-FTIR. The absorption spectra of the plasma polymerization amine-containing functional layers in nitrogen-containing plasma are shown in Fig. 2. The presence of functional amine groups on NH_3 + He and N_2 + He plasma treated PS was indicated by the peak of the primary amine ($-NH_2$) stretching absorption at the 3,440 cm^{-1} region and the C–N stretching absorption at the 1,267 cm^{-1} region. The aromatic ring of PS structure is indicated by the peak of the absorption at the 1,598 cm^{-1} region (Birgit et al. 2007; Lizhen et al. 2010). The following FTIR spectrographic facts were used to explain the weak peak of N–H and C–N in Fig. 2. These peaks are only a guide to the chemical composition of the plasma-modified surface. The detected signals were always lower than the actual amount, because the layers of N–H and C–N formed were very thin (Jinmo et al. 2007). However, in combination with the XPS result, it can be clearly seen

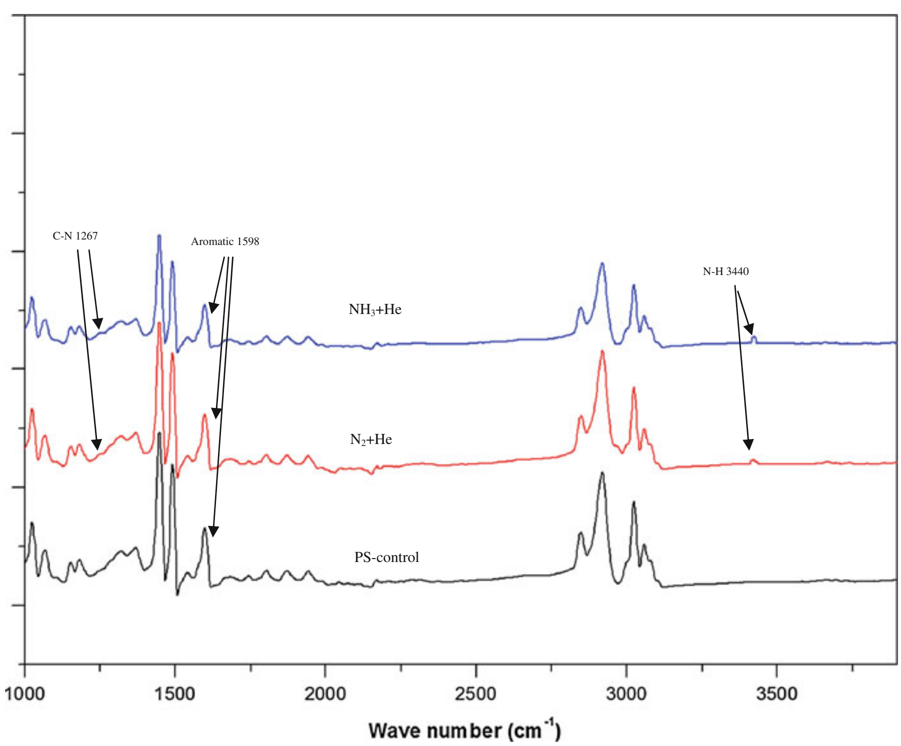

Fig. 2 FTIR spectrum of the plasma treatment amine-containing functional groups with PS-control, N_2 + He and NH_3 + He treated PS-membrane

that up to 9 % of functional groups were replaced on the PS surface. On the other hand, amine signals on the treated PS surface were from the gas phase treatment. No residual gas without chemical reaction was left on the surface after that. Anyway, if there should be some non-covalently-bound amine on the surface, they would have been taken away by the rigorously ethanol and ultrasonic cleaning, which was carried out after the plasma treatment.

On the XPS analysis, we considered and discussed our results here in relation to several previous studies (Lizhen et al. 2010; Grazia et al. 2009; Zi-Xing et al. 2010). XPS characterizes the treated surfaces to obtain the information on chemical structure. Figure 3 shows the survey scan spectra of PS-control, N_2 + He treated PS-membrane and NH_3 + He treated PS-membrane. The survey spectra confirmed the presence of C1 s and O1 s on PS-control, demonstrating the oxygen-containing pretreatment onto the PS surface and the presence of C1s, O1s and N1s of treated PS-membranes. Figure 4 shows high-resolution C1s (Fig. 4a) spectra of PS-control, C1s (Fig. 4b) of N_2-treated PS-membrane, C1s (Fig. 4c) of NH_3-treated PS-membrane, N1s (Fig. 4d) of N_2-treated PS-membrane and N1s (Fig. 4e) of NH_3-treated PS-membrane. The C1s peak of PS-control was deconvoluted into five peaks with binding energies of 284.6, 285.2, 285.9, 286.7 and 291.3 eV, which were attributed to carbons in C–C or C–H, C=C, C–H_2, C–O or C–OH and π–π*, respectively (Fig. 4a) (Yasushi et al. 2008). The π–π* C1s peak is due to "shake-up" excitations taking place in the π orbitals on the benzene rings. NH_3-treated PS-membrane produced two new peaks with binding energies of 287.7 and 288.6 eV, which were attributed to C=O and N–C=O (amide) groups, respectively (Fig. 4b). In addition, two peaks were identified of N1s spectra shown in Fig. 4e. The peak at 398.5 eV was assigned to N=C or NH_2 bonds and peak at 400.5 eV was assigned to NHC=O, NH_2 or N–H of NH_3^+ (Birgit et al. 2007; Jinmo et al. 2007). N_2-treated PS-membrane produced two peaks with binding energies of 287.7 and 288.6 eV same as NH_3-treated PS-membrane but N1s spectra was deconvoluted into one peak with binding energies of 400.3 eV.

Table 2 summarizes the results of a deconvolution analysis of C1s peaks, shown in Fig. 4. The NH_3 plasma and N_2 plasma were successfully N-functionalized on PS surface and a larger amount of oxygen functional groups and nitrogen functional groups were introduced by NH_3 plasma than by N_2 plasma, because the C1s peak at 285.0–286.9 eV assigned to C–O, C–N, C=N and C≡N bonds was significantly increased when observed in the NH_3 plasma-treated PS-membrane, indicating the formation of functional carbonyl, amide and amine groups on membrane surface, especially with NH_3 plasma.

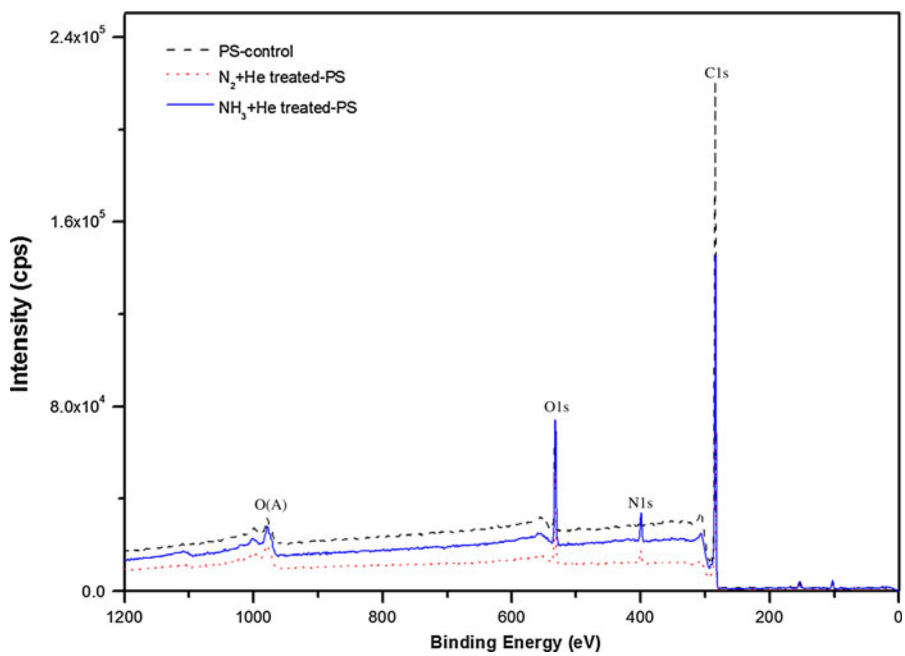

Fig. 3 XPS scan spectra of PS-control, N_2 + He treated PS-membrane and NH_3 + He treated PS-membrane

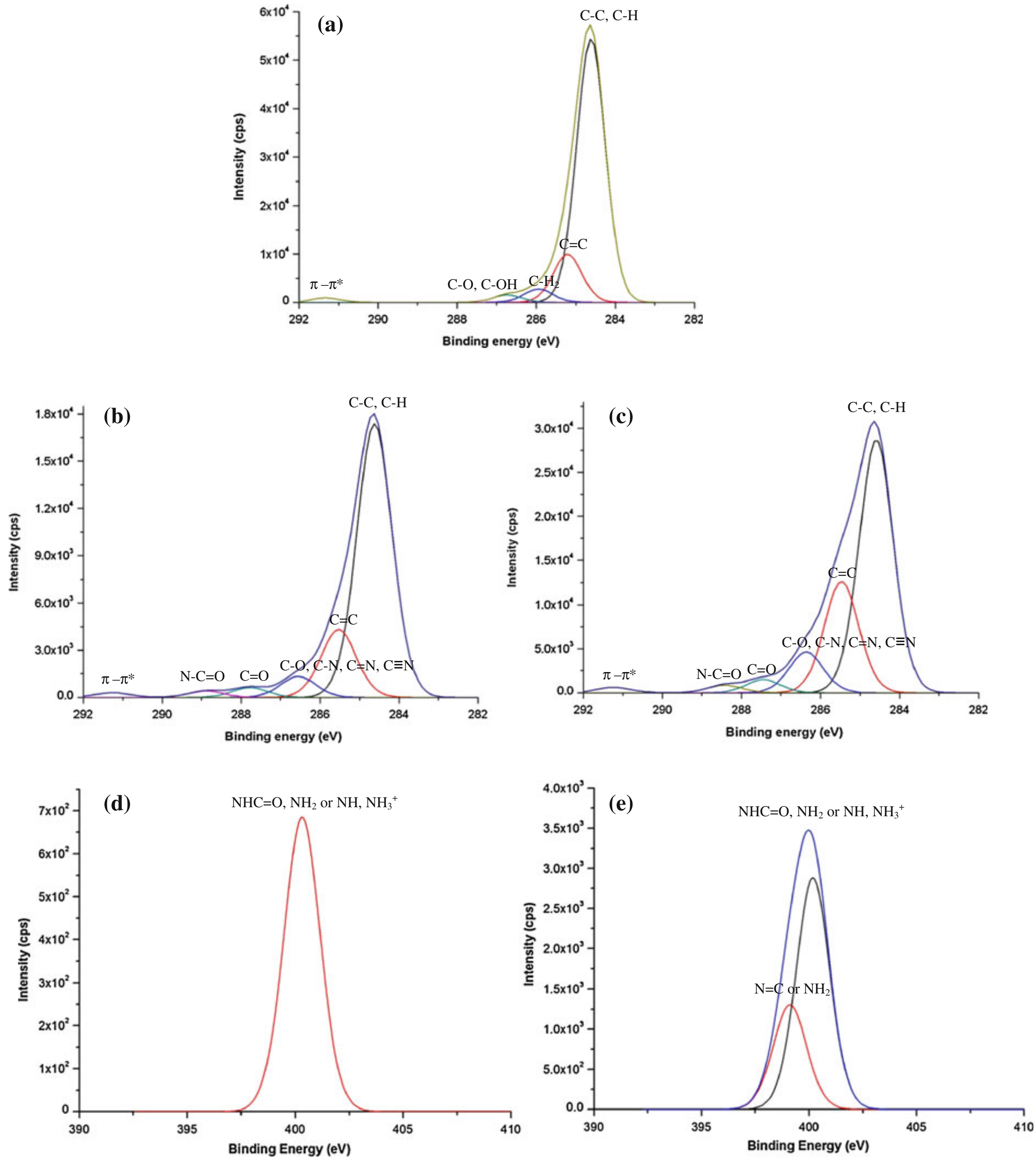

Fig. 4 High resolution peaks of C1s for PS control (**a**), N_2 + He treated PS-membrane (**b**), NH_3 + He treated PS-membrane (**c**) and N1s for N_2 + He treated PS-membrane (**d**) and NH_3 + He treated PS-membrane (×20 of **d**) (**e**)

Cell behavior

Cell behavior experiments were performed over 7 days using BCP-K1. Figure 5 shows the percentage of attached cells on the PS-membrane samples when cultured for 1 day. Compared with cells from the PS-control group, almost all groups of cells on the treated PS-membrane showed a significantly increased

Table 2 Estimated percentage of carbon functional groups from C1s XPS spectra

PS sample	Binding energy (eV)	Assignments	Peak area (%)
PS control	284.6	C–C, C–H	78.2
	285.2	C=C	14.4
	285.9	$-CH_2-$	4.0
	286.7	C–O, C–OH	2.2
	291.3	π–π*	1.2
NH_3-treated PS	284.6	C–C, C–H	78.3
	285.6	C=C	11.4
	286.5	C–O, C–N, C=N, C≡N	4.5
	287.7	C=O	2.7
	288.6	N–C=O amide	1.6
	291.3	π–π*	1.2
N_2-treated PS	284.6	C–C, C–H	79.6
	285.6	C=C	10.3
	286.5	C–O, C–N, C=N, C≡N	4.4
	287.6	C=O	2.4
	288.7	N–C=O amide	2.2
	291.1	π–π*	1.1

adhesion, especially the mixed-He groups. Less adhesion was observed on the two groups of mixed-Ar at 50 W ($p \leq 0.01$). In addition, BCP-K1 tended to proliferate and spread over surfaces of PS-membranes at the 50 W N_2 + He, 100 W NH_3 + Ar and 100 W NH_3 + He when cultured for 3, 5 and 7 days as shown in Fig. 6. The relative percentage of cell proliferation on the PS-control exhibited only 80 on day 7 compared with day 1. In contrast, cell proliferation on the treated PS-membrane samples increased about 150 on day 7 compared with those on day 1. The plasma treatments of 50 W N_2 + He and 100 W NH_3 + He were, therefore, chosen for further study since they were the best two treatments of PS surface, in terms of cell adhesion and proliferation efficiency. Note that measurement of water contact angle (Table 1) was carried out immediately after surface preparation, under the dry surface conditions. Submerging the surface into the culture medium over the 7 days experiment (Fig. 6) caused the "hydrophobic recovery" and also a "decay effect" (Fig. 1) and eventually resulted in cell proliferation. Furthermore, BCP-K1 showed very good attachment on NH_3 + He 50 or 100 W surface at day 1 (Fig. 5), but showed less ability to proliferate by day 7 (Fig. 6). It was possible that the culture medium and culture conditions over the 7 days of cell culture caused leakage of functional groups, due to "hydrophobic recovery" and also the "decay effect". Ar and He are precursor gases to assist and retain plasma condition (Hiraoka et al. 2004). Neither of them alone generated amines on the treated surfaces (Junyou et al. 2005; Naveed et al. 2006) and they were therefore not evaluated for cell behavior in this experiment.

Cell adhesion and proliferation was observed by light microscope and photomicrographs taken in the serial time courses as shown in Fig. 7. The photomicrographs

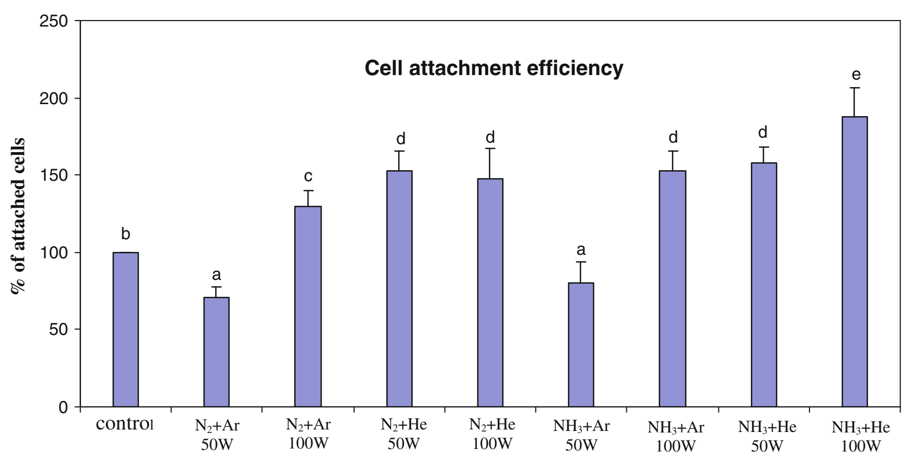

Fig. 5 Attachment efficiency of BCP-K1 on PS surfaces when cultured for 1 day. The data were calculated and converted to percentages (mean ± SD). Different letters above the bars indicate significant differences at $p \leq 0.05$

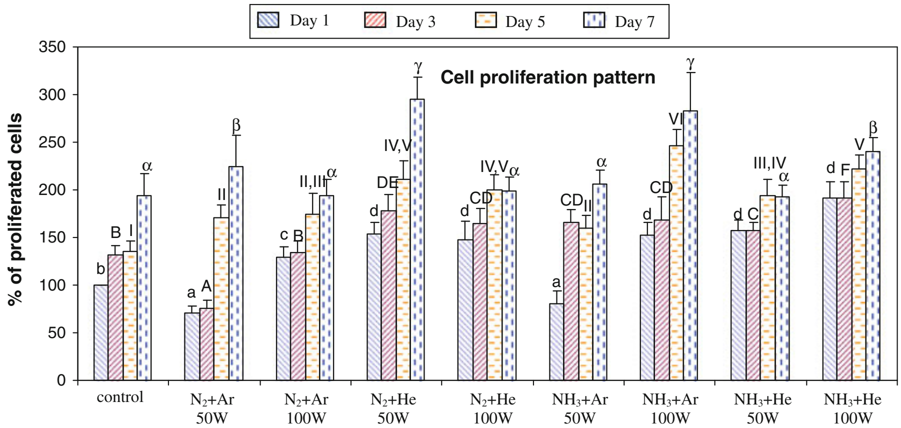

Fig. 6 Cell proliferation patterns of BCP-K1 on PS surfaces when cultured for 1, 3, 5 and 7 days. The *letters* on the *bar top* indicate the same result within 5 % ($p \leq 0.05$). (*a*, *b*, *c*, and *d* are on day 1, *A*, *B*, *C*, *D*, *E*, and *F* are on day 3, *I*, *II*, *III*, *IV*, and *V* are on day 5, and α, β, and γ are on day 7 of culturing)

clearly displayed more cells on the treated PS-membrane than on the PS-control, indicating more effective cell adhesion and enhanced proliferation on the treated PS-membrane than the commercialized PS-controls. Furthermore, cells attached to all treated PS-membrane surfaces exhibited normal fibroblast-like morphology similar to those on the PS-controls.

Cellular behavior on any biomaterial is an important indication to determine its biocompatibility. The whole process of adhesion and spreading of cells after contact with biomaterials consists of cell attachment, filopodia growth, cytoplasmic webbing and flattening cell mass, and the ruffling of peripheral cytoplasm, which progress in a sequential fashion (Dadsetan et al. 2001). As seen in Fig. 8, the typical SEM images along the time courses showed different attachment of cells on different PS surfaces. Cells on the treated PS-membrane surfaces adhered and spread more than on the PS-control surfaces. Incomplete attachment of BCP-K1, with ragged cytoplasmic boundary, was often observed on the PS-control surfaces at day 1.

Focal adhesion kinase is an integrin, involved in multi-protein complex formation, which links ECM to the actin cytoskeleton and related signaling proteins. FAK is also involved in the regulation of cellular migration, proliferation, survival and invasion in some cell types (Venkata et al. 2010). Examination of FAK indicates cellular adhesion, proliferation and spreading on the PS surfaces. Figure 9 shows the amount of FAK protein as the OD_{492} value, i.e., the higher the OD value, the greater is the amount of FAK protein secreted from the cells. Considering the two patterns of FAK amount exhibited among the PS surfaces. Firstly, at day 1 and 7, the significantly highest FAK was observed on the cells adhered to the 50 W N_2 + He-treated PS-membrane, while the cells on the 100 W NH_3 + He-treated PS-membrane secreted similar amounts of FAK as the PS-control. This display might imply that the N_2 + He-treated PS-membrane enhanced more cellular activities related to FAK secretion than the other surfaces. Apparently, such cellular activities on day 1 and 7 were not activated during day 3 and 5, when significant similarities appeared among the three types of surfaces. It is possible that the FAK might be activated via different pathways and play different roles (Lim et al. 2008; Hall et al. 2011). Secondly, the secreted FAK on day 3 and 5 was significantly less than on days 1 and 7, indicating the similar pattern of cellular activities on the PS surfaces. This FAK pattern (Fig. 9) supported the explanation of related proliferation behaviors of the cell along the time courses (Fig. 6). Considering day 1, the cells needed FAK for initial attachment and that raised the total amount of secreted FAK. On days 3–5, the cells underwent a lag period of intracellular growth adjustment, almost without proliferation; hence the lower amount of FAK. On day 7, the cells regained their activity, entering exponential growth phase and recommenced FAK secretion. This explained the FAK amount, related to the pattern of MSC growth, similar to other cell types in vitro (Lee et al. 2004; Bonab et al. 2006).

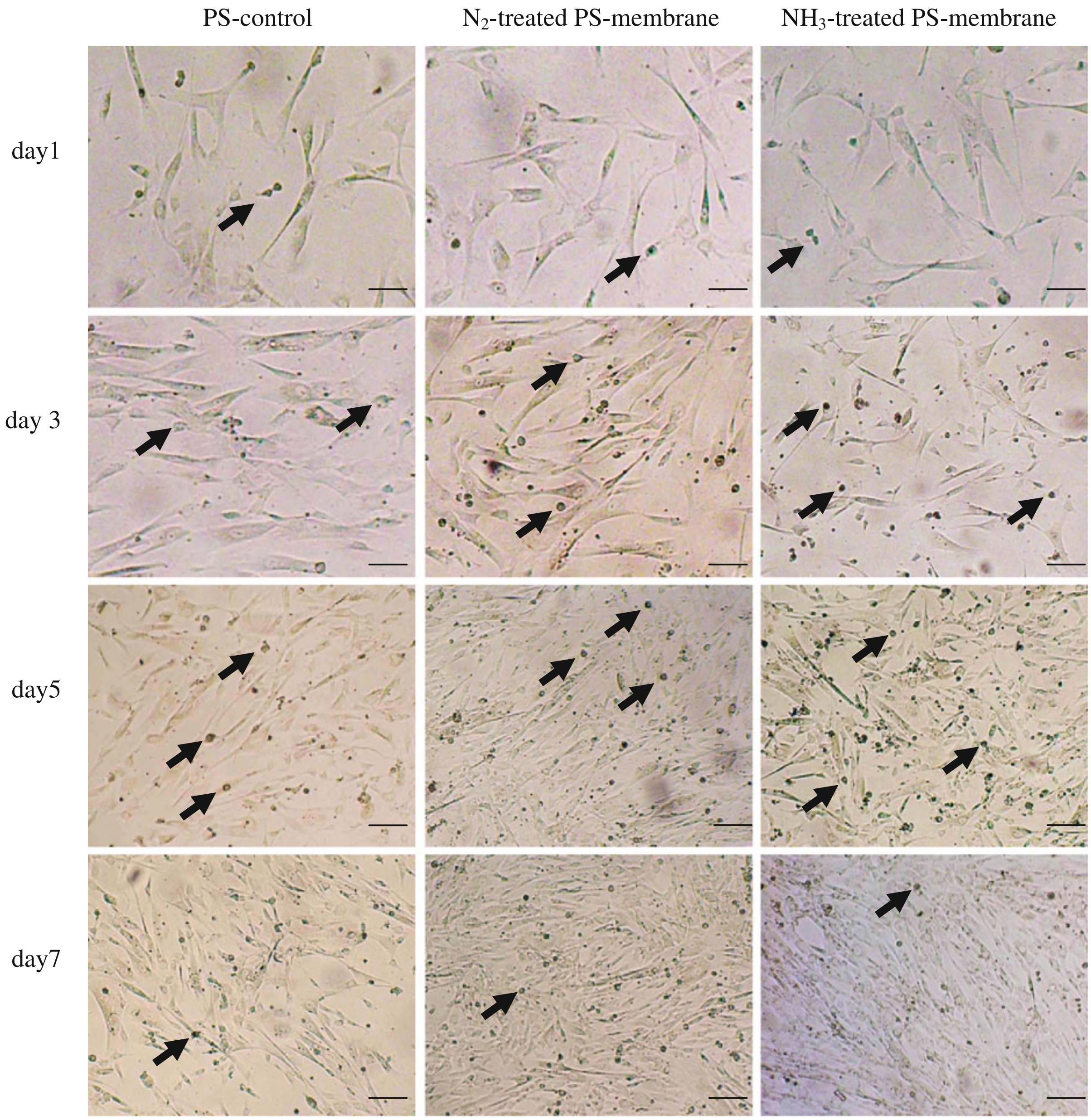

Fig. 7 Optical micrographs of attachment and proliferation of BCP-K1 when cultured on PS-control, 50 W N_2 + He treated PS-membrane and 100 W NH_3 + He treated PS-membrane for 1, 3, 5 and 7 days. Dividing cells could be seen as many small spherical spots (sample at *arrow point*) during day 3 and 5, but with less number on day 1 and 7. (*Scale bar* = 100 μm)

From immunocytochemical analysis, the stemness markers were performed to monitor the stability of BCP-K1 on the three types of PS surfaces used. Cells on all PS surfaces were positive for mesenchymal stem cell marker; CD105, undifferentiated WJMSC markers, CD9, and SSEA-4 and negative for heamatopoietic stem cell marker; CD34. This result agrees with Alaminos et al. (2010), who reported expression of the major characteristic criterion of human mesenchymal stem cell (hMSC). The samples of fluorescent photomicrography from this experiment are shown in Fig. 10.

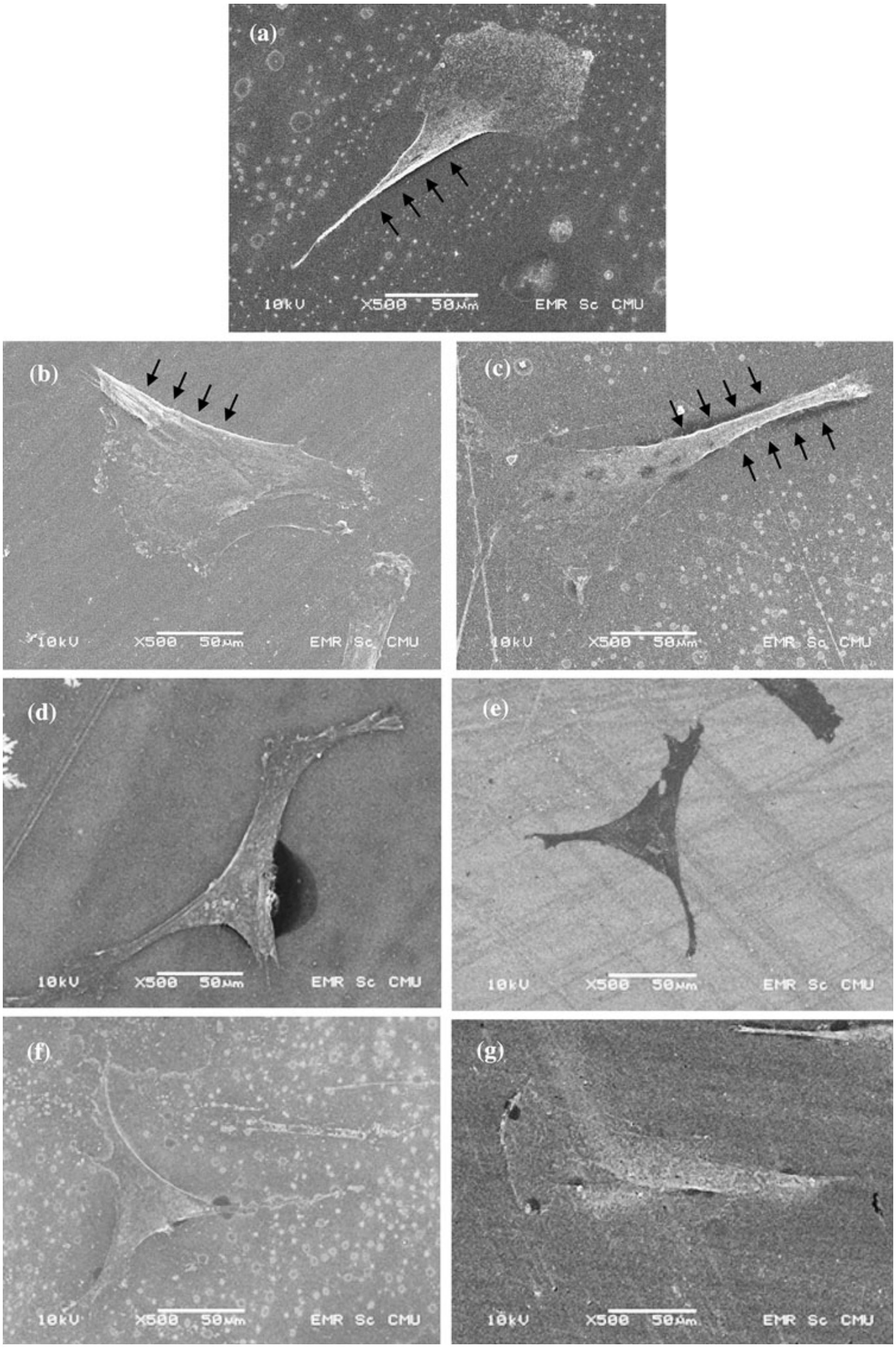

Fig. 8 Example of SEM micrographs of attachment of BCP-K1 when cultured on PS-control (**a**, **b**, **c**), N_2 + He treated PS-membrane (**d**, **e**) and NH_3 + He treated PS-membrane (**f**, **g**) for 24 h. On PS-control surface, ragged boundary (*arrows*) was often seen among cells, indicating the incomplete attachment. (*Scale bar* = 50 μm)

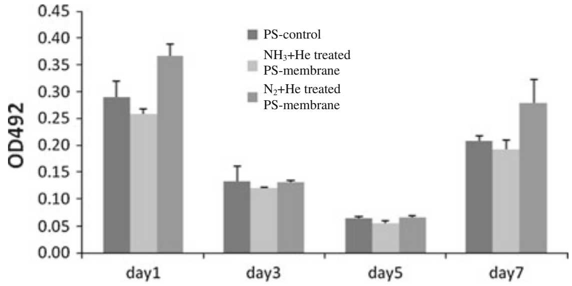

Fig. 9 FAK-ELISA of BCP-K1 culturing on different PS samples for 1, 3, 5 and 7 days (mean ± SD)

Conclusion

In this study, the surface properties of PS-membrane samples were successfully modified with nitrogen- and ammonia-containing plasma, to deposit functional groups onto the membrane surface. Stability of amine functional groups on the PS surface was achieved, using mixtures of N_2 + He or NH_3 + He gas. He plasma created stable covalent binding sites for attachment of amine functional groups. Cellular adhesion and proliferation were significantly improved as well as stemness stability. Results were explained by changes in wettability and surface functionalization and the creation of functional carbonyl, amide and amine groups on the PS surface. Stability of the plasma-treated surface was achieved via crosslinked polymers, using N-containing gas mixed with He gas. The present findings provide a guideline for surface modification of PS culture vessels, for biomedical applications.

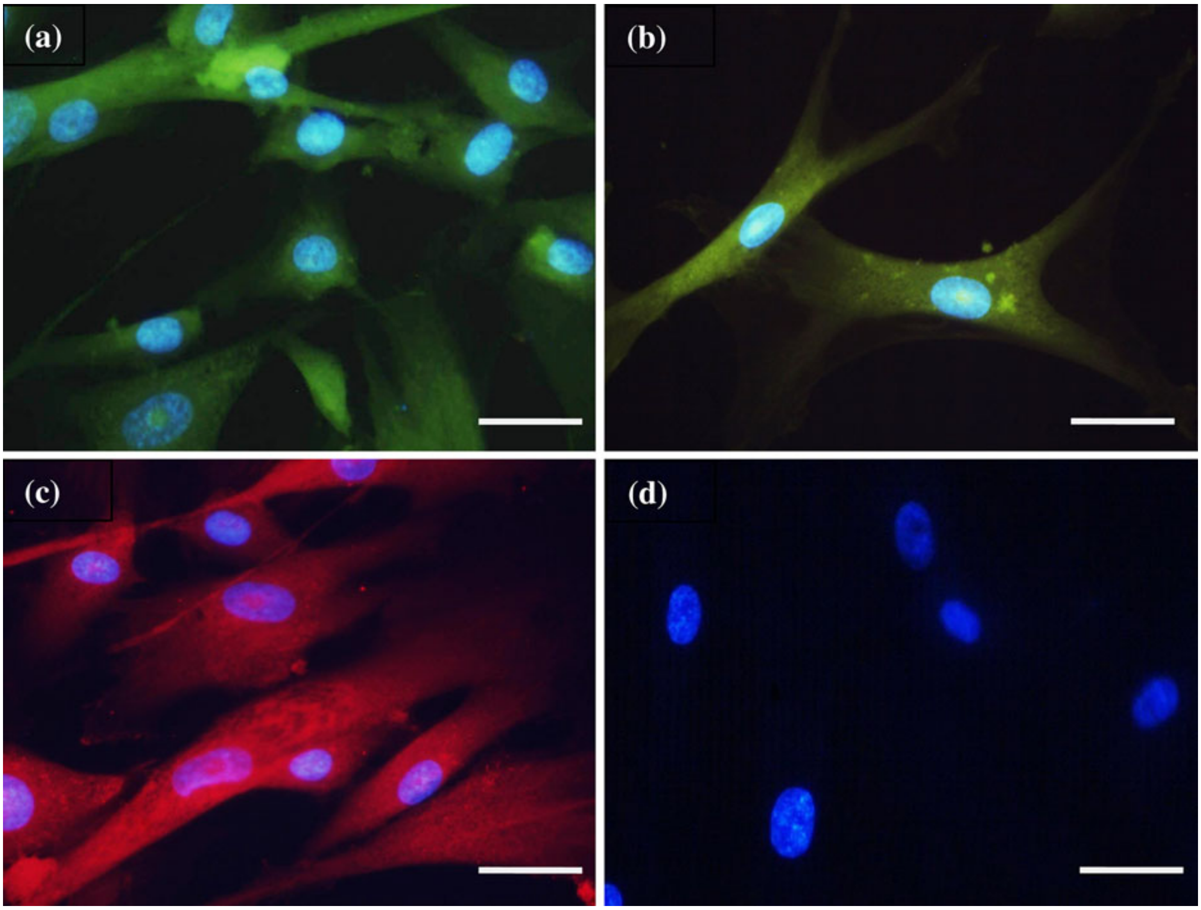

Fig. 10 Immunocytochemical analysis of BCP-K1 for (**a**) the mesenchymal stem cell markers, CD105, (**b**) undifferentiated WJMSC markers, CD9, and (**c**) SSEA-4. Negative result (**d**) for hematopoietic stem cell marker, CD34, showed *blue nuclei* from DAPI. (Alexa Fluor®488: *green*, Alexa Fluor®546: *yellow*, Alexa Fluor®594: *red*, DAPI: *blue*) (*scale bar* = 100 μm). (Color figure online)

Acknowledgments We thank the National Research University (NRU) Project under Thailand's Office of the Higher Education Commission (OHEC), the Graduate School Chiang Mai University and Thailand Center of Excellence in Physics (ThEP) for financial and scholarship support.

References

Alaminos M, Pérez-Köhler B, Garzón I, García-Honduvilla N, Romero B, Campos A, Buján J (2010) Transdifferentiation potentiality of human Wharton's jelly stem cells towards vascular endothelial cells. J Cell Physiol 223:640–647

Amstein CF, Hartman PA (1975) Adaptation of plastic surfaces for tissue culture by glow discharge. J Clin Microbiol 2:46

Arefi-Khonsari M, Mabille-Rouger F, Amouroux I, Gheorgiu J, Bouchier M (1995) Role of helium plasma pretreatment in the stability of the wettability, adhesion, and mechanical properties of ammonia plasma- treated polymers. J Adhes Sci Technol 9:923–934

Bacakova L, Filova E, Parizek M, Ruml T, Svorcik V (2011) Modulation of cell adhesion, proliferation and differentiation on materials designed for body implants. Biotechnol Adv 29:739–767

Baksh D, Yao R, Tuan RS (2007) Comparison of proliferative and multilineage differentiation potential of human mesenchymal stem cells derived from umbilical cord and bone marrow. Stem Cells 25:1384–1392

Baksh D, Song L, Tuan R (2008) Adult mesenchymal stem cells: characterization, differentiation, and application in cell and gene therapy. J Cell Mol Med 8:301–316

Barbash IM, Chouraqui P, Baron J, Feinberg MS, Etzion S, Tessone A, Miller L, Guetta E, Zipori D, Kedes LH (2003) Systemic delivery of bone marrow-derived mesenchymal stem cells to the infarcted myocardium: feasibility, cell migration, and body distribution. Circulation 108:863

Bell KL, Dalgarno A, Kingston AE (1968) Penning ionization by metastable helium atoms. J Phys B: At Mol Opt Phys 1:18

Birgit F, Frank L, Karsten S, Petra DM, Claudia B, Marion F, Andreas O, Barbara JN (2007) The effect of positively charged plasma polymerization on initial osteoblastic focal adhesion on titanium surfaces. Biomaterials 28:4521–4534

Bonab M, Alimoghaddam K, Talebian F, Ghaffari S, Ghavamzadeh A, Nikbin B (2006) Aging of mesenchymal stem cell in vitro. BMC Cell Biol 7:14

Brohlin M, Mahay D, Novikov LN, Terenghi G, Wiberg M, Shawcross SG, Novikova LN (2009) Characterisation of human mesenchymal stem cells following differentiation into Schwann cell-like cells. Neurosci Res 64:41–49

Chaiwong C, Rachtanapun P, Wongchaiya P, Auras R, Boonyawan D (2010) Effect of plasma treatment on hydrophobicity and barrier property of polylactic acid. Surf Coat Technol 204:2933–2939

Chen J, Li Y, Wang L, Zhang Z, Lu D, Lu M, Chopp M (2001) Therapeutic benefit of intravenous administration of bone marrow stromal cells after cerebral ischemia in rats. Stroke 32:1005

Dadsetan M, Mirzadeh H, Sharifi N, Daliri M (2001) Cell behavior on laser surface-modified polyethylene terephthalate in vitro. J Biomed Mater Res A 57:183–189

Docheva D, Popov C, Mutschler W, Schieker M (2007) Human mesenchymal stem cells in contact with their environment: surface characteristics and the integrin system. J Cell Mol Med 11:21–38

Dupont-Gillain CC, Adriaensen Y, Derclaye S, Rouxhet P (2000) Plasma-oxidized polystyrene: wetting properties and surface reconstruction. Langmuir 16:8194–8200

Gerritsen C, Allan SH, Jan F (1995) Introduction of functional groups on polyethylene surfaces by a carbon dioxide plasma treatment. J Appl Polym Sci 57:969–982

Granchelli J (2009) Surface innovation: optimising cell adhesion. Cell culture, drug discovery focus (ARLSPBTISURF 77817). http://www.nuncbrand.com/files/en-12068.pdf. Accessed 15 Oct 2011

Grazia MLM, Cristina S, Giovanni M (2009) A multitechnique study of preferential protein adsorption on hydrophobic and hydrophilic plasma-modified polymer surfaces. Colloids Surf B Biointerfaces 70:76–83

Grinnell F (1978) Cellular adhesiveness and extracellular substrata. Int Rev Cytol 53:65–144

Hall J, Fu W, Schaller M (2011) Chapter five—focal adhesion kinase: exploring FAK structure to gain insight into function. In: Kwang WJ (ed) International review of cell and molecular biology, vol. 288, ISBN 1937-6448, Academic Press, London, pp 185–225

Hiraoka K, Fujimaki S, Kambara S, Furuya H, Okazaki S (2004) Atmospheric-pressure penning ionization mass spectrometry. Rapid Commun Mass Spectrom 18:2323–2330

Ji G-Z, Wei X, Chen G-Q (2009) Growth of human umbilical cord Wharton's jelly-derived mesenchymal stem cells on the terpolyester poly(3-hydroxybutyrate-co-3-hydroxyvalerate-co-3-hydroxyhexanoate). J Biomater Sci Polym Ed 20:325–339

Jinmo K, Donggeun J, Yongsup P, Yongki K, Dae WM, Tae GL (2007) Quantitative analysis of surface amine groups on plasma-polymerized ethylenediamine films using UV–visible spectroscopy compared to chemical derivatization with FT-IR spectroscopy, XPS and TOF-SIMS. Appl Surf Sci 253:4112–4118

Junyou L, Fengjiu S, Hanjiang Y (2005) Enhancement of the molecular nitrogen dissociation and ionization levels by argon mixture in flue nitrogen plasma. Curr Appl Phys 5:625–628

Kim J, Chaudhury MK, Owen MJ (2000) Hydrophobic recovery of polydimethylsiloxane elastomer exposed to partial electrical discharge. J Colloid Interface Sci 226:231–236

Kim SS, Leanne B, Sunil K, Hans JG (2006) Plasma methods for the generation of chemically reactive surfaces for biomolecule immobilization and cell colonization-a review. Plasma Process Polym 3:392–418

Koh S-H, Kim KS, Choi MR, Jung KH, Park KS, Chai YG, Roh W, Hwang SJ, Ko H-J, Huh Y-M et al (2008) Implantation of human umbilical cord-derived mesenchymal stem cells as a neuroprotective therapy for ischemic stroke in rats. Brain Res 1229:233–248

Kubota S (1970) Non-metastable penning effect in the alpha-particle ionization of inert gas mixtures. J Phys Soc Jpn 29:1017–1029

Lee R, Kim B, Choi I, Kim H, Choi H, Suh K, Bae Y, Jung J (2004) Characterization and expression analysis of

mesenchymal stem cells from human bone marrow and adipose tissue. Cell Physiol Biochem 14:311–324
Lim S, Chen X, Lim Y, Hanson D, Vo T, Howerton K, Larocque N, Fisher S, Schlaepfer D, IIic D (2008) Nuclear FAK promotes cell proliferation and survival through FERM-Enhanced p53 degradation. Mol Cell 29:9–22
Lizhen Y, Juan L, Zhenduo W, Zhongwei L, Qiang C (2010) Calibration of amine density measurement on plasma grafting PET surface and its cell adsorption behaviour. Surf Coat Tech 205:S345–S348
Maroudas NG (1977) Sulphonated polystyrene as an optimal substratum for the adhesion and spreading of mesenchymal cells in monovalent and divalent saline solutions. J Cell Physiol 90:511–519
Naveed MA, Qayyum A, Shujaat A, Zakaullah M (2006) Effects of helium gas mixing on the production of active species in nitrogen plasma. Phys Lett A 359:499–503
Prockop DJ (2004) Time to end the stem cell wars? Blood 104:3421
Riccardi C, Roman HE, Ziano R (2010) Attachment of polymer chains on plasma-treated surfaces: experiments and modeling. New J Phys 12: 073008 (12 pp)
Ronald CC, Ximing X, Thomas RG, Hans JG (1995) Quantitative analysis of polymer surface restructuring. Langmuir 11:2576–2584
Rubin H (1966) Altering bacteriological plastic petri dishes for tissue culture use. USPHS Rep 81:843–844
Sarugaser R, Lickorish D, Baksh D, Hosseini MM, Davies JE (2005) Human umbilical cord perivascular (HUCPV) cells: a source of mesenchymal progenitors. Stem Cells 23:220–229
Skarlatos SI, Rao R, Kruth HS (1992) Accelerated development of human monocyte-macrophages cultured on Plastek-C tissue culture dishes. Method Cell Sci 14:113–117
Teare D, Emmison N, Ton-That C, Bradley R (2000) Cellular attachment to ultraviolet ozone modified polystyrene surfaces. Langmuir 16:2818–2824
Troyer DL, Weiss ML (2008) Concise review: Wharton's jelly derived cells are a primitive stromal cell population. Stem Cells 26:591–599
Truica-Marasescu F, Girard-Lauriault PL, Lippitz L, Unger WES, Wertheimer MR (2008) Nitrogen-rich plasma polymers: comparison of films deposited in atmospheric- and low-pressure plasma. Thin Solid Films 516:7406–7417
Van Kooten TG, Spijker HT, Busscher HJ (2004) Plasma-treated polystyrene surfaces: model surfaces for studying cell-biomaterial interactions. Biomaterials 25:1735–1747
Venkata RD, Kiranpreet K, Kiran KV, Dzung HD, Andrew JT, Sanjeeva M, Jasti SR(2010) Downregulation of Focal Adhesion Kinase (FAK) by cord blood stem cells inhibits angiogenesis in glioblastoma. Aging (Albany NY): 791–803
Veronis G, Inan US, Pasko VP (2000) Fundamental properties of inert gas mixtures for plasma display panels. IEEE Trans Plasma Sci 28:1271–1279
Wagner W, Wein F, Seckinger A, Frankhauser M, Wirkner U, Krause U, Blake J, Schwager C, Eckstein V, Ansorge W (2005) Comparative characteristics of mesenchymal stem cells from human bone marrow, adipose tissue, and umbilical cord blood. Exp Hematol 33:1402–1416
Yasushi S, Natsuko M, Shin-ichi K, Masayuki K (2008) Introduction of carboxyl group onto polystyrene surface using plasma techniques. Surf Coat Tech 202:5724–5727
Yuk-Hong T, Chi-Chun L, Sang-Min P, Hongquan J, Paul FN, Amy EW (2010) Surface roughening of polystyrene and poly(methyl methacrylate) in Ar/O_2 plasma etching. Polymer 2:649–663
Zhang M, Mal N, Kiedrowski M, Chacko M, Askari AT, Popovic ZB, Koc ON, Penn MS (2007) SDF-1 expression by mesenchymal stem cells results in trophic support of cardiac myocytes after myocardial infarction. FASEB J 21:3197
Zi-Xing X, Tao L, Zhao-Ming Z, Ding-Sheng Z, Song-Hui W, Fu-Qiang L, Wen-De X, Xiao-Rui J, Xin-Xin Z, Jian-Ting C (2010) Amide-linkage formed between ammonia plasma treated poly(D, L-lactide acid) scaffolds and bio-peptides: enhancement of cell adhesion and osteogenic differentiation in vitro. Biopolymers 95:682–694